

Fermi Surface of CeIn₃ above the Néel Critical Field

| | |
|-------|--|
| メタデータ | 言語: en 出版者: American Physical Society 公開日: 2008-02-25 キーワード (Ja): キーワード (En): 作成者: Harrison, N., Sebastian, Suchitra E., Mielke, C. H., Paris, A., Gordon, M. J., Swenson, C. A., Rickel, D. G., Pacheco, M. D., Ruminer, P. F., Schillig, J. B., Sims, J. R., Lacerda, A. H., Suzuki, M.-T., Harima, H., Ebihara, Takao メールアドレス: 所属: |
| URL | http://hdl.handle.net/10297/596 |

Fermi Surface of CeIn₃ above the Néel Critical Field

N. Harrison,¹ S. E. Sebastian,² C. H. Mielke,¹ A. Paris,¹ M. J. Gordon,¹ C. A. Swenson,¹ D. G. Rickel,¹ M. D. Pacheco,¹ P. F. Ruminer,¹ J. B. Schillig,¹ J. R. Sims,¹ A. H. Lacerda,¹ M.-T. Suzuki,³ H. Harima,³ and T. Ebihara⁴

¹National High Magnetic Field Laboratory, Los Alamos National Laboratory, MS E536, Los Alamos, New Mexico 87545, USA

²Cavendish Laboratory, University of Cambridge, Madingley Road, Cambridge CB3 0HE, United Kingdom

³Department of Physics, Kobe University, Kobe 657-8501, Japan

⁴Department of Physics, Shizuoka University, Shizuoka 422-8529, Japan

(Received 16 April 2007; published 31 July 2007)

We report measurements of the de Haas–van Alphen effect in CeIn₃ in magnetic fields extending to ≈ 90 T, well above the Néel critical field of $\mu_0 H_c \approx 61$ T. The unreconstructed Fermi surface *a* sheet is observed in the high magnetic field polarized paramagnetic limit, but with its effective mass and Fermi surface volume strongly reduced in size compared to that observed in the low magnetic field paramagnetic regime under pressure. The spheroidal topology of this sheet provides an ideal realization of the transformation from a “large Fermi surface” accommodating *f* electrons to a “small Fermi surface” when the *f*-electron moments become polarized.

DOI: 10.1103/PhysRevLett.99.056401

PACS numbers: 71.18.+y, 71.27.+a, 75.20.Hr, 75.30.Fv

Strong magnetic fields are an indispensable tool for studying the energy scales relevant to antiferromagnetism. By polarizing their magnetic moments, they deplete the system of available spin degrees of freedom for staggered ordering. In *f*-electron antiferromagnets, polarization is expected to be accompanied by the effective removal of the *f*-electron degrees of freedom from the Fermi surface (FS) [1–3], enabling access to the underlying electronic structure in its simplest form. The *f*-electron system CeIn₃ provides an essential paradigm to understand universal aspects of the relationship between antiferromagnetism and unconventional superconductivity—given the magnetic simplicity of this nonmetamagnetic cubic system [2,4] compared with CeRu₂Si₂ [5], CeB₆ [6], or CeRhIn₅ [7]. Universal behavior is realized in CeIn₃ by the application of pressure, whereupon antiferromagnetism is suppressed and superconductivity [8] and heavy fermion behavior emerge [9]. If NdB₆ provides a model example of a cubic system in which the hybridization between the *f* electrons and conduction electrons remains negligible throughout [10], then CeIn₃ may be considered as the model system for understanding antiferromagnetism preceding superconductivity in the opposite strongly correlated regime comprising heavy quasiparticles [11,12].

One unavoidable consequence of a monotonic nonmetamagnet magnetization is that much stronger magnetic fields are required to polarize the quasiparticle bands to suppress the correlations [13,14]. In CeIn₃ this requires exceeding the critical field of the Néel ordered phase, $\mu_0 H_c \approx 61$ T [4]. To determine the electronic structure of CeIn₃ in magnetic fields above H_c , we use the recently constructed 100 T magnet at Los Alamos [15]—presently delivering magnetic fields of up to 90 T (see Fig. 1) while being commissioned. Measurements of the de Haas–van Alphen (dHvA) effect over a wide interval in field above H_c enable the unreconstructed FS of CeIn₃ to be observed

in the polarized state, and compared with that previously observed in the paramagnetic regime at pressures exceeding the critical pressure $p_c \approx 26$ kbar [9].

The magnetic field \mathbf{H} is generated in two stages. First, a 1.4 GW motor generator is used to energize an “outsert” coil, delivering a ≈ 36 T “base” magnetic field in a 0.2 m bore. A 2.5 MJ capacitor bank is then used to energize an “insert” coil to produce the remaining ≈ 54 T in a 15 mm bore [16]. Figure 1(a) shows an example of the total magnetic field-versus-time profile experienced by the CeIn₃ samples studied in this Letter. With the exception of the magnetic field generation, the dHvA experimental technique is identical to that used in regular pulsed magnetic field experiments [4,10,17]. Three single crystalline CeIn₃ samples are cut and etched to diameters of less than 300 μm for experiments with $\mathbf{H} \parallel \langle 100 \rangle$, $\langle 110 \rangle$, and $\langle 111 \rangle$. The dHvA effect is measured using a coaxially arranged

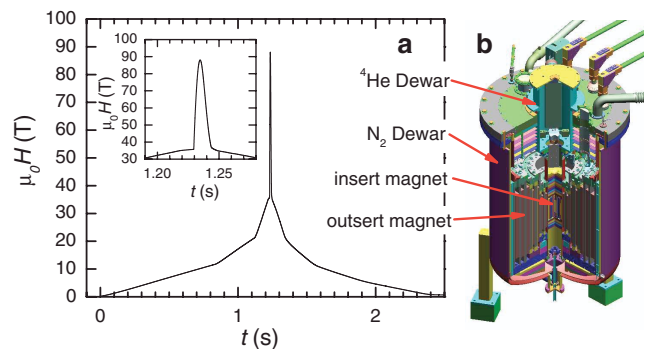


FIG. 1 (color). (a) The H -versus-time T profile of the pulse generated by the combined “outsert” and “insert” magnets. The inset shows the region of the pulse profile provided by the insert magnet in which dHvA measurements in Fig. 2 are made. (b) A schematic of the magnet used for generating the pulse (outer diameter ≈ 1.4 m).

compensated pair of detection coils with the innermost coil having ≈ 460 turns and an inner bore of $450 \mu\text{m}$. A digitizer captures the dHvA signal data while temperatures between 300 mK and 4 K are obtained by controlling the vapor pressure of liquid ^3He and ^4He reservoirs.

Figure 2 shows examples of dHvA signals and Fourier transforms for $\mathbf{H} \parallel \langle 100 \rangle$ and $\langle 110 \rangle$. For $\mathbf{H} \parallel \langle 100 \rangle$, the signal is dominated by the d branch in both the antiferromagnetic ($\mu_0 H < \mu_0 H_c \approx 61$ T) and polarized paramagnetic regimes ($H > H_c$). The n frequency [11] is also observed to appear prominently at high magnetic fields. The a sheet (see Fig. 3) yields a relatively weak feature corresponding to a large electron sheet centered at the R point of the Brillouin zone [18], observable above the level of noise over a restricted interval 75–85 T in magnetic fields (see Fig. 3). This frequency becomes more prominent for $\mathbf{H} \parallel \langle 110 \rangle$ (Fig. 2, lower panel) and $\langle 111 \rangle$, appearing at all fields $\mu_0 H \gtrsim 55$ T.

Fermi surface measurements of Ce compounds are often reported to be consistent with either of two dichotomous scenarios. In one scenario, good agreement is found with band structure calculations in which the f -electron shells are completely filled or empty, as for the Lu and La analog compounds, indicating that the f electrons contribute negligibly to the FS volume. A compound with these characteristics is considered to have a “small FS” (i.e., the FS is much smaller than it might otherwise be were the f elec-

trons to contribute their charge degrees of freedom) [19]. In the other scenario, some level of agreement is found with band structure calculations in which the f electrons are treated as band electrons. A compound with these characteristics is then considered to have a “large FS” (see Fig. 4) [19]. Our present measurements outside the antiferromagnetic phase of CeIn_3 reveal that both these scenarios are realized in the same isotropic material under conditions of either extreme pressure [9] or intense magnetic field. dHvA measurements made at $p > p_c$ are consistent with band structure calculations in which the f electrons are treated as itinerant, as shown in Fig. 3 [18]. Satisfactory agreement requires the effects of Coulomb repulsion and the orbital manifold of the lowest lying Γ_7 doublet to be taken into consideration [18]. Our high magnetic field a -sheet measurements on CeIn_3 (see Fig. 3), in contrast, are found to be similar to the predicted electronic structure of LuIn_3 , which has filled f shells. CeIn_3 therefore provides a particularly clear example of a system in which a transformation occurs from a “large FS” at high pressures and low magnetic fields to a “small FS” at high magnetic fields and ambient pressure. Since CeIn_3 is nonmetamagnetic [2,4] and it is possible (in principle) to move from the high pressure regime to the high magnetic field regime without

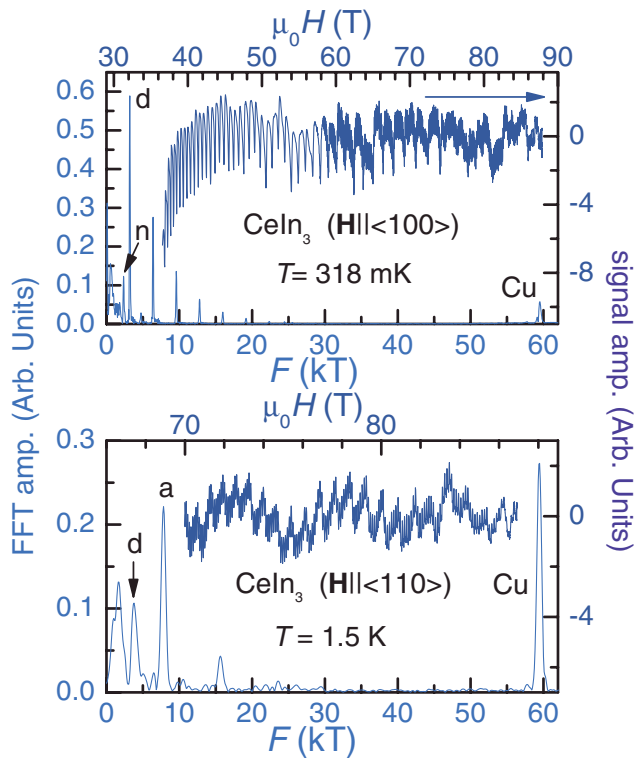


FIG. 2 (color). Examples of dHvA signal measurements on CeIn_3 for two different orientations of \mathbf{H} together with Fourier transforms. The Cu signal originates from the polycrystalline Cu comprising the detection coils.

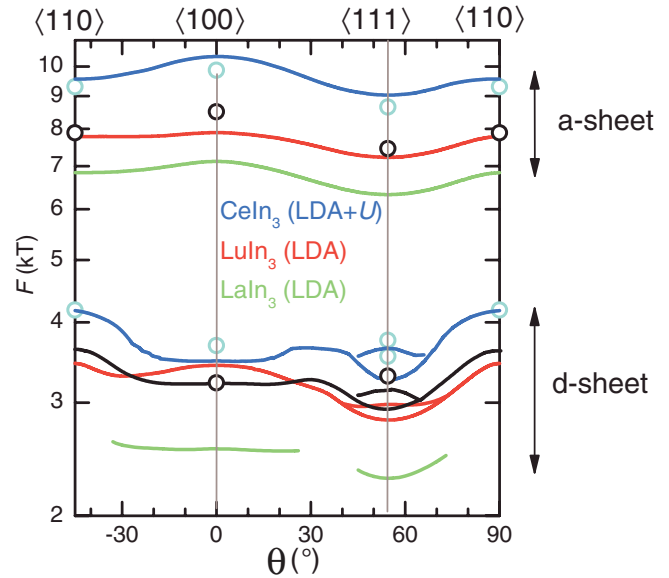


FIG. 3 (color). A comparison of the d - and a -sheet FS's of CeIn_3 measured at ambient pressure and 27 kbar with those calculated for CeIn_3 (blue lines), LuIn_3 (red lines) and LaIn_3 (green lines) using the local density approximation (LDA) method (inclusive of the Coulomb interaction U in the case of CeIn_3 [18]). Black lines indicate the magnetic field-orientation dependence of the d sheet obtained by Endo *et al.* [11], revealing a close similarity to that of LuIn_3 . Black open circles represent the a and d sheets observed by us in strong magnetic fields and ambient pressure, while cyan circles represent the d and a sheets measured by Settai *et al.* for $p > p_c$ [9]. Measured frequencies are constant to within 1% between 50 and 90 T.

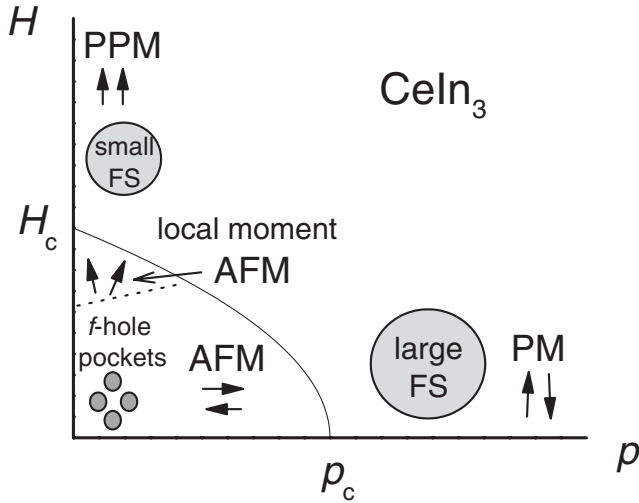


FIG. 4. A schematic p versus H phase diagram of CeIn_3 , including the antiferromagnetic (AFM), paramagnetic (PM), and polarized paramagnetic (PPM) regimes. Solid arrows represent the spin states of the Γ_7 doublet of Ce in each of these regimes, while the gray circles represent the different FS's. The “large FS” includes f -electron charge degrees of freedom whereas the “small FS” does not. Small f -hole pockets have recently been observed inside the antiferromagnetic phase at ambient pressure [12], but are observed to become depopulated in magnetic fields above ≈ 41 T (dotted line) where the staggered moment is canted.

crossing the antiferromagnetic phase boundary, the transformation in FS must take place in a continuous fashion.

The present experimental limitations require us to study the link between the high pressure and high magnetic field regimes via the intervening antiferromagnetic phase. The manner in which each section of the FS is modified by the antiferromagnetic order parameter depends on its size, location in \mathbf{k} space, and the extent to which it accommodates f electrons. The d sheet passes through H_c and p_c in Fig. 4 relatively unperturbed in topology or effective mass [9,18], as indicated in Figs. 2 and 5(a). This robustness to antiferromagnetism and high magnetic fields arises from the minimal contribution of the f electrons to the d -sheet volume (the f -electron dispersion exhibits a minimum at the Γ point in the Brillouin zone [18]), and its small size well within the interior of the antiferromagnetic Brillouin zone.

The a sheet, by contrast, is radically affected by antiferromagnetism owing to its much greater size and hybridization with the f dispersion near the Fermi energy. The large size of the staggered moment within the antiferromagnetic phase of CeIn_3 [20], combined with the weak dispersion of the f band in the paramagnetic phase [18], requires the antiferromagnetism to be considered from the strong coupling perspective [12]. The disappearance of the a sheet at pressures $p < p_c$ [9] reflects the effective removal of the majority of the f electrons from the FS deep within the antiferromagnetic phase, where strong coupling

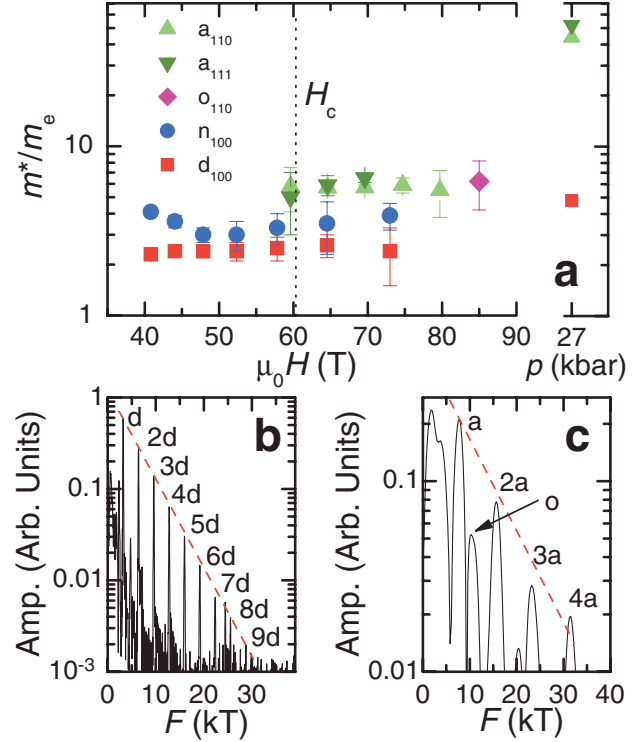


FIG. 5 (color). (a) Effective masses of different extremal dHvA orbits in CeIn_3 , estimated by fitting the Lifshitz-Kosevich theoretic form to the temperature dependence of the quantum oscillation amplitude measured between 300 mK and 4 K. The subscript in the legend refers to the orientation of \mathbf{H} . Masses for the same orbits measured at $p > p_c$ by Settai *et al.* are shown to the right for comparison. (b) Part of the $\mathbf{H} \parallel (100)$ Fourier transform from Fig. 2 plotted on a logarithmic scale so as to show the exponential dependence of the d_{100} frequency harmonics on harmonic index. The red dotted line is a guide to the eye. (c) A similar Fourier transform for the a_{110} frequency, performed over a restricted interval in magnetic field 80–87 T where the harmonic content is most pronounced.

gaps the f -electron dispersion. Unlike the d -sheet FS, the evolution of the a -sheet FS topology cannot easily be predicted in the intermediate regime close to the antiferromagnetic boundary where local staggered moment ordering competes with Kondo screening [21]. A clearer picture begins to emerge in high magnetic fields once the hybridization becomes perturbatively weak due to the field-induced polarization of the quasiparticle bands (as with the suppression of Kondo screening deep within the antiferromagnetic phase [12]). The effective mass of the a sheet in Fig. 5(a) is observed to be magnetic field independent (within experimental error) and roughly an order of magnitude smaller than that observed at $p > p_c$, providing compelling evidence for the removal of the majority of the f electrons from this sheet due to the field-induced polarization of the quasiparticle bands [3]. While the experimental picture at low magnetic fields and ambient pressure is more complex, with small pockets of f holes [12] coexisting with fragments of the unhybridized

conduction band FS resembling LuIn_3 , magnetic breakdown tunneling at higher magnetic fields causes the reemergence of this a sheet at fields slightly below H_c .

Spin-dependent effective masses are another consequence of the polarization of the f electrons in strong magnetic fields. In the case of the d_{100} frequency, shown in Fig. 5(b), the absence of a significant f -electron contribution causes the spin dependence to closely mimic the localized f -electron behavior seen in the single impurity limit, as realized in $\text{Ce}_x\text{La}_{1-x}\text{B}_6$ [17] and $\text{Ce}_x\text{La}_{1-x}\text{RhIn}_5$ [22] for $x \lesssim 10\%$. Localization of the f electrons causes the spin-up and spin-down dHvA frequencies to be the same, but with the lighter mass spin component dominating the dHvA signal, causing the harmonic index dependence of the dHvA amplitude to decay in a simple exponential manner. In the case of the a_{110} frequency, four harmonics are observed at the highest magnetic fields, $80 < \mu_0 H < 87$ T, in Fig. 5(c). The observed field independence of the a -sheet FS topology and effective mass suggests that the polarization of the quasiparticle bands is more complete than realized in CeB_6 and CeRu_2Si_2 , where well separated dHvA frequencies corresponding to split spin-up and spin-down Fermi surfaces and/or field-dependent effective masses are observed [5,23]. Exchange splitting effects caused by the polarized f moments (as in NdB_6 [10,24]) can also not be resolved at high magnetic fields in CeIn_3 . The new o_{110} frequency (and its harmonic) at $\approx 10\,400$ T in Fig. 5(c) has a similar size to other features predicted in the LuIn_3 band structure calculations [25].

In summary, we observe the a -sheet FS of CeIn_3 in strong magnetic fields $H > H_c$, which is found to be consistent with the “small FS” picture [19], in which the f electrons do not contribute significantly to its volume, in contrast to that observed within the paramagnetic regime at pressures $p > p_c$. Consequently, its effective mass is observed to be reduced by an order of magnitude compared to that at $p > p_c$. The spheroidal geometry of the FS represents an ideal embodiment of the change in the electronic structure from large FS (at high pressure) to a small FS (in strong magnetic fields). Although a direct observation of this transformation is presently masked by the intervening antiferromagnetic phase, the transformation is expected to take place continuously given the cubic symmetry of CeIn_3 [2] (the absence of metamagnetism is already established at ambient pressure [4]). The present experiments on CeIn_3 show the importance of extreme experimental conditions for understanding electronic structure of strongly correlated f -electron metals.

This work was performed under the auspices of the National Science Foundation, the Department of Energy (U.S.), and Florida state. T.E. acknowledges support provided by a Grant-in-Aid for Scientific Research on priority Areas, “High Field Spin Science in 100 T” (CASIO) and MEXT. S.E.S. acknowledges support from the Institute

for Complex Adaptive Matter and from Trinity College, Cambridge University.

-
- [1] A. Wasserman, M. Springford, and A. C. Hewson, *J. Phys. Condens. Matter* **1**, 2669 (1989).
 - [2] S. M. M. Evans, *Europhys. Lett.* **17**, 469 (1992).
 - [3] D. M. Edwards and A. C. M. Green, *Z. Phys. B* **103**, 243 (1997).
 - [4] T. Ebihara *et al.*, *Phys. Rev. Lett.* **93**, 246401 (2004).
 - [5] Strong anisotropy of the hybridization between the f electrons and the conduction electrons is required to explain metamagnetism in CeRu_2Si_2 in the absence of magnetic ordering [2].
 - [6] Metamagnetism in CeB_2 is caused by a transition between antiferromagnetic and antiferroquadrupolar phases (otherwise unexpected in a cubic system [2]); R. G. Goodrich *et al.*, *Phys. Rev. B* **69**, 054415 (2004).
 - [7] The upper critical field of the antiferromagnetic phase of CeRhIn_5 appears to coincide with metamagnetism, possibly as a consequence of the anisotropy of the crystal electric fields in the tetragonal symmetry; T. Takeuchi *et al.*, *J. Phys. Soc. Jpn.* **70**, 877 (2001).
 - [8] N. D. Mathur *et al.*, *Nature (London)* **394**, 39 (1998).
 - [9] R. Settai *et al.*, *J. Phys. Soc. Jpn.* **74**, 3016 (2005).
 - [10] R. G. Goodrich, N. Harrison, and Z. Fisk, *Phys. Rev. Lett.* **97**, 146404 (2006).
 - [11] M. Endo, N. Kimura, and H. Aoki, *J. Phys. Soc. Jpn.* **74**, 3295 (2005).
 - [12] S. E. Sebastian *et al.* (unpublished); Effective masses as large as 100 times the free electron mass m_e are observed in fields approaching ≈ 41 T.
 - [13] J. A. Detwiler *et al.*, *Phys. Rev. B* **61**, 402 (2000).
 - [14] T. Sakakibara *et al.*, *J. Magn. Magn. Mater.* **70**, 375 (1987).
 - [15] J. L. Bacon *et al.*, *IEEE Trans. Appl. Supercond.* **12**, 695 (2002).
 - [16] C. A. Swenson *et al.*, *Physica (Amsterdam)* **346B–347B**, 561 (2004).
 - [17] N. Harrison *et al.*, *Phys. Rev. Lett.* **81**, 870 (1998); A. A. Teklu *et al.*, *Phys. Rev. B* **62**, 12 875 (2000).
 - [18] M.-T. Suzuki, Ph.D. thesis, Kobe University, 2007; M.-T. Suzuki and H. Harima, *Physica B (Amsterdam)* (to be published).
 - [19] P. Coleman *et al.*, *J. Phys. Condens. Matter* **13**, R723 (2001).
 - [20] J. M. Lawrence and S. M. Shapiro, *Phys. Rev. B* **22**, 4379 (1980).
 - [21] Q. M. Si, *Physica (Amsterdam)* **378B**, 23 (2006).
 - [22] U. Alver *et al.*, *Phys. Rev. B* **64**, 180402 (2001).
 - [23] This is evidenced by recent observations of a new frequency α' , smaller and heavier than that of the α_1 frequency, but corresponding to the same topology, as revealed by its angular dependence; M. Endo *et al.*, *J. Phys. Soc. Jpn.* **75**, 114704 (2006).
 - [24] L. P. Gor'kov and P. D. Grigoriev, *Phys. Rev. B* **73**, 060401 (2006).
 - [25] H. Harima (private communication).